

A UNIFIED IMEX RUNGE–KUTTA APPROACH FOR HYPERBOLIC SYSTEMS WITH MULTISCALE RELAXATION*

SEBASTIANO BOSCARINO[†], LORENZO PARESCHI[‡], AND GIOVANNI RUSSO[†]

Abstract. In this paper we consider the development of Implicit-Explicit (IMEX) Runge–Kutta schemes for hyperbolic systems with multiscale relaxation. In such systems the scaling depends on an additional parameter which modifies the nature of the asymptotic behavior, which can be either hyperbolic or parabolic. Because of the multiple scalings, standard IMEX Runge–Kutta methods for hyperbolic systems with relaxation lose their efficiency, and a different approach should be adopted to guarantee asymptotic preservation in stiff regimes. We show that the proposed approach is capable of capturing the correct asymptotic limit of the system independently of the scaling used. Several numerical examples confirm our theoretical analysis.

Key words. IMEX Runge–Kutta methods, hyperbolic conservation laws with sources, diffusion equations, hydrodynamic limits, stiff systems, asymptotic-preserving schemes

AMS subject classifications. 65C20, 65M06, 76D05, 82C40

DOI. 10.1137/M1111449

1. Introduction. Hyperbolic systems with relaxation often contain multiple space-time scales which may differ by several orders of magnitude due to the various physical parameters characterizing the model. This is the case, for example, with kinetic equations close to the hydrodynamic limit [4, 14, 12]. In such regimes these systems can be more conveniently described in terms of fluid-dynamic equations when they are considered on a suitable space-time scale.

As a prototype system that we will use to illustrate the subsequent theory, we consider the following:

$$(1) \quad \begin{cases} \partial_t u + \partial_x v = 0, \\ \partial_t v + \frac{1}{\varepsilon^{2\alpha}} \partial_x p(u) = -\frac{1}{\varepsilon^{1+\alpha}} (v - f(u)), \quad \alpha \in [0, 1], \end{cases}$$

where $p'(u) > 0$. System (1) is hyperbolic with two distinct real characteristic speeds $\pm \sqrt{p'(u)/\varepsilon^\alpha}$.

Note that the scaling introduced in (1) corresponds to the study of the limiting behavior of the solution for the usual hyperbolic system with a singular perturbation

*Received by the editors January 17, 2017; accepted for publication (in revised form) June 20, 2017; published electronically August 31, 2017.

<http://www.siam.org/journals/sinum/55-4/M111144.html>

Funding: The work of the authors was partially supported by the grant *Numerical Methods for Uncertainty Quantification in Hyperbolic and Kinetic Equations* of the group GNCS of INdAM, by the ITN-ETN Marie-Curie Horizon 2020 program ModCompShock, *Modeling and Computation of Shocks and Interfaces*, Project ID: 642768, and by the INDAM-GNCS 2017 research grant *Numerical Methods for Hyperbolic and Kinetic Equation and Applications*.

[†]Department of Mathematics and Computer Science, University of Catania, Catania, Italy (boscarino@dmi.unict.it, <http://www.dmi.unict.it/~boscarino/>, russo@dmi.unict.it, <http://www.dmi.unict.it/~russo/>).

[‡]Department of Mathematics and Computer Science, University of Ferrara, Ferrara, Italy (lorenzo.pareschi@unife.it, <http://www.lorenzopareschi.com/>).

source,

$$(2) \quad \begin{cases} \partial_\tau u + \partial_\xi V = 0, \\ \partial_\tau V + \partial_\xi p(u) = -\frac{1}{\varepsilon} (V - F(u)), \end{cases}$$

under the rescaling $t = \varepsilon^\alpha \tau$, $\xi = x$, $v(x, t) = V(\xi, \tau)/\varepsilon^\alpha$, and $f(u) = F(u)/\varepsilon^\alpha$.

For $\alpha = 0$, system 1 reduces to the usual hyperbolic scaling (2). However, if $\alpha > 0$, we are looking at larger microscopic times.

In particular, for small values of ε , using the Chapman–Enskog expansion, the behavior of the solution to (1) is, at least formally, governed by the following nonlinear parabolic equation:

$$(3) \quad \begin{cases} v = f(u) - \varepsilon^{1-\alpha} \partial_x p(u) + \varepsilon^{1+\alpha} f'(u)^2 \partial_x u + \mathcal{O}(\varepsilon^2), \\ \partial_t u + \partial_x f(u) = \varepsilon^{1+\alpha} \partial_x \left[\left(\frac{p'(u)}{\varepsilon^{2\alpha}} - f'(u)^2 \right) \partial_x u \right] + \mathcal{O}(\varepsilon^2). \end{cases}$$

Therefore, as $\varepsilon \rightarrow 0$ when $\alpha \in [0, 1)$, we obtain the scalar conservation law

$$(4) \quad \begin{cases} v = f(u), \\ \partial_t u + \partial_x f(u) = 0. \end{cases}$$

Note that the main stability condition [13, 28] for system (3) corresponds to

$$(5) \quad f'(u)^2 < \frac{p'(u)}{\varepsilon^{2\alpha}},$$

and it is always satisfied in the limit $\varepsilon \rightarrow 0$ when $\alpha > 0$, whereas for $\alpha = 0$ it requires suitable assumptions on the functions $f(u)$ and $p(u)$.

In classical kinetic theory the space-time scaling just discussed leads to the so-called hydrodynamical limits of the Boltzmann equation (see [12, Chapter 11]). For $\alpha = 0$ this corresponds to the *compressible Euler limit*, whereas for $\alpha \in (0, 1)$ the *incompressible Euler limit* is obtained.

Something special happens when $\alpha = 1$. In this case, in fact, to leading order in ε , we obtain the parabolic equation

$$(6) \quad \begin{cases} v = f(u) - \partial_x p(u), \\ \partial_t u + \partial_x f(u) = \partial_{xx} p(u). \end{cases}$$

In other words, considering times larger than those typical for Euler dynamics ($\alpha = 1$ instead of $\alpha \in [0, 1)$), dissipative effects become nonnegligible. This behavior characterizes the *incompressible Navier–Stokes limit* in classical kinetic theory.

The development of numerical methods to solve hyperbolic systems with stiff source terms in the case when $\alpha = 0$ has been an active area of research in the past three decades [10, 22, 18, 31, 33, 34, 32, 7]. Another series of works is concerned with the construction of robust schemes for $\alpha = 1$ when a diffusion limit is obtained [21, 23, 25, 26]. However, very few papers have considered the general multiscale problem of type (1) for the various possible values of α [29, 24].

The common goal of this general class of methods, often referred to as *asymptotic-preserving* (AP) schemes, is to obtain the macroscopic behavior described by the equilibrium system by solving the original relaxation system (1) with coarse grids $\Delta t, \Delta x \gg \varepsilon$, where Δt and Δx are, respectively, the time step and the mesh size.

Note that since the characteristic speeds of the hyperbolic part of system (1) are of order $1/\varepsilon^\alpha$, most of the popular methods [10, 22, 32] for the solution to hyperbolic conservation laws with stiff relaxation present several limitations when considering the whole range of $\alpha \in [0, 1]$ and fail to capture the right behavior of the limit equilibrium equation unless the small relaxation rate is numerically resolved, leading to a stability condition of the form $\Delta t \sim \varepsilon^\alpha \Delta x$. Clearly, this *hyperbolic stiffness* becomes very restrictive when $\alpha > 0$, and for $\alpha = 1$ in the parabolic regime $\varepsilon \ll \Delta x$, where for an explicit scheme a parabolic time step restriction of the type $\Delta t \sim \Delta x^2$ is expected. A special class of Implicit-Explicit (IMEX) schemes with explicit flux and implicit relaxation is able to deal with the parabolic relaxation ($\alpha = 1$) [8]. Such methods, however, converge to an explicit scheme for the limit parabolic equation, thus requiring a penalization technique to remove the final parabolic stiffness [6, 8, 9].

In the present paper, using a reformulation of the problem, we develop high-order IMEX Runge–Kutta schemes for a system like (1) in the stiff regime which work uniformly with respect to the scaling parameter α . In the parabolic regime, $\alpha = 1$, our approach gives a scheme which is not only consistent with (6) without resolving the small ε scale, but is also capable of avoiding the *parabolic stiffness* leading to the CFL condition $\Delta t \sim \Delta x^2$. In other limiting regimes, that is to say, when $\alpha \in [0, 1)$, the scheme maintains all the nice properties of the numerical schemes for hyperbolic conservation laws, such as the ability to capture shocks with high resolution.

Here, although the final schemes we develop will work independently on ε , we will mainly concentrate on the study of the stiff regime for system (1), that is to say, when $\varepsilon \ll 1$.

Finally we emphasize that from a physical point of view the problem we consider here is close in spirit to the description of the macroscopic incompressible Navier–Stokes equations of fluid-dynamics by way of detailed kinetic equations [4, 14, 12]. Although, for the sake of simplicity, we develop our theory for one-dimensional 2×2 systems, the results extend far beyond these models.

The rest of this paper is organized as follows. In section 2 we recall some of the most popular IMEX Runge–Kutta approaches and emphasize their limited applicability when α ranges on the whole $[0, 1]$ interval. Next, in section 3 we introduce our new approach with the aim of avoiding the stiffness induced by the characteristic speeds of system (1). First, we present the simple first order scheme and then, using the IMEX Runge–Kutta formalism, we construct high order methods. In the case when $\alpha = 1$, these methods give rise to an explicit approximation of the limiting parabolic problem. In section 4 we modify the previous schemes in order to avoid the limiting parabolic stiffness. In these schemes the diffusion term in the limiting equation is integrated implicitly. Finally, in section 5 several numerical examples are presented showing the robustness of the present approach. Some final considerations are contained in the last section and an appendix is also included.

2. Previous IMEX Runge–Kutta approaches. In this section, to motivate the new approach, we recall briefly other ways to tackle stiff problems through an IMEX partitioning of the differential system.

We discretize time first, and then we discretize space on the time discrete scheme. The motivation for not adopting a method of line approach is that we can choose the space discretization most suitable for each term. For simplicity of notation, in what

follows we assume that $\alpha = 1$, and consider the hyperbolic-to-parabolic relaxation. Similar conclusions are obtained for $\alpha \in (0, 1)$. Considerations on the case $\alpha = 0$ are reported at the end of each subsection.

2.1. Additive approach. Let us consider the simple IMEX Euler method as applied to (1), based on taking the fluxes explicitly and the stiff source implicitly [32]:

$$(7) \quad \begin{aligned} \frac{u^{n+1} - u^n}{\Delta t} &= -v_x^n, \\ \varepsilon^2 \frac{v^{n+1} - v^n}{\Delta t} &= -p(u^n)_x - (v^{n+1} - f(u^{n+1})). \end{aligned}$$

Solving the second equation for v^{n+1} one obtains

$$(8) \quad v^{n+1} = \frac{\varepsilon^2}{\varepsilon^2 + \Delta t} v^n - \frac{\Delta t}{\varepsilon^2 + \Delta t} (p(u^n)_x - f(u^{n+1})).$$

Making use of this relation (replacing n by $n - 1$) in the first equation, we get

$$\frac{u^{n+1} - u^n}{\Delta t} + \frac{\varepsilon^2}{\varepsilon^2 + \Delta t} v_x^{n-1} = \frac{\Delta t}{\varepsilon^2 + \Delta t} (p(u^{n-1})_{xx} - f(u^n)_x).$$

Therefore, in the limit $\varepsilon \rightarrow 0$, we have a two level scheme (in time) for problem (6),

$$(9) \quad \frac{u^{n+1} - u^n}{\Delta t} = p(u^{n-1})_{xx} - f(u^n)_x.$$

Although (9) is a consistent time discretization of the limit convection-diffusion equation (6), the presence of the term u^{n-1} degrades the accuracy of the first order scheme.

Furthermore, since as $\varepsilon \rightarrow 0$ the equilibrium state of (8)

$$v^{n+1} = f(u^{n+1}) - p(u^n)_x$$

involves two time levels, in general additional conditions on the explicit and implicit schemes are necessary in order to obtain asymptotic preserving high order methods. We refer to [8] for more details. These drawbacks are also present for any value of $\alpha \in (0, 1]$. Of course, since the additive approach has been originally designed to deal with the case $\alpha = 0$, there are no problems in the regime.

2.2. Partitioned approach. A different way to apply the IMEX Euler method to (1) is based on taking the first equation explicitly and the second implicitly [5, 6, 30]:

$$(10) \quad \begin{aligned} \frac{u^{n+1} - u^n}{\Delta t} &= -v_x^n, \\ \varepsilon^2 \frac{v^{n+1} - v^n}{\Delta t} &= -p(u^{n+1})_x - (v^{n+1} - f(u^{n+1})). \end{aligned}$$

Solving for v^{n+1} , the second equation we get is

$$(11) \quad v^{n+1} = \frac{\varepsilon^2}{\varepsilon^2 + \Delta t} v^n - \frac{\Delta t}{\varepsilon^2 + \Delta t} (p(u^{n+1})_x - f(u^{n+1})),$$

which substituted into the first equation results in the two level scheme

$$\frac{u^{n+1} - u^n}{\Delta t} + \frac{\varepsilon^2}{\varepsilon^2 + \Delta t} v_x^{n-1} = \frac{\Delta t}{\varepsilon^2 + \Delta t} (p(u^n)_{xx} - f(u^n)_x).$$

Of course, since the method has been developed specifically for the case when $\alpha = 1$, in the limit $\varepsilon \rightarrow 0$ it yields a consistent explicit scheme for problem (6),

$$(12) \quad \frac{u^{n+1} - u^n}{\Delta t} = p(u^n)_{xx} - f(u^n)_x.$$

It is easy to verify that this approach also gives a consistent explicit scheme for any value of $\alpha \in [0, 1)$ in the hyperbolic limit. However, for nonvanishing small values of ε , the discretization of the fluxes at different time levels poses several difficulties. For example, if we consider for simplicity $p'(u) = 1$, introducing the diagonal variables $u \pm \varepsilon v$, system (10) reads

$$(13) \quad \begin{aligned} \frac{(u^{n+1} + \varepsilon v^{n+1}) - (u^n + \varepsilon v^n)}{\Delta t} &= -\frac{1}{\varepsilon}(u^{n+1} + \varepsilon v^n)_x - \frac{1}{\varepsilon}(v^{n+1} - f(u^{n+1})), \\ \frac{(u^{n+1} - \varepsilon v^{n+1}) - (u^n - \varepsilon v^n)}{\Delta t} &= +\frac{1}{\varepsilon}(u^{n+1} - \varepsilon v^n)_x + \frac{1}{\varepsilon}(v^{n+1} - f(u^{n+1})), \end{aligned}$$

and therefore, the space derivatives of diagonal variables in (13) are defined as a combination of two time levels, and it is then not clear how to discretize the system in characteristic variables. Furthermore, most numerical methods based on conservative variables evaluate the flux at the same time level. We refer to [6] for a discussion on these aspects and extensions to schemes that avoid the parabolic stiffness in the relaxation limit for $\alpha = 1$.

2.3. Hybrid additive-partitioned approach. A method which combines the advantages of the previous approaches in the various regimes has been proposed in [25, 26]. The idea is to take a convex combination of the previous schemes in such a way that we have an additive scheme in hyperbolic regimes and a partitioned one in parabolic regimes. This is achieved by taking

$$(14) \quad \begin{aligned} \frac{u^{n+1} - u^n}{\Delta t} &= -v_x^n, \\ \varepsilon^2 \frac{v^{n+1} - v^n}{\Delta t} &= -\phi(\varepsilon)p(u^n)_x - (1 - \phi(\varepsilon))p(u^{n+1})_x - (v^{n+1} - f(u^{n+1})), \end{aligned}$$

where $0 \leq \phi(\varepsilon) \leq 1$ is such that $\phi(\varepsilon) \approx 1$ for $\varepsilon = \mathcal{O}(1)$ and $\phi(\varepsilon) \approx 0$ when $\varepsilon \ll 1$. For example $\phi(\varepsilon) = \min\{\varepsilon^2, 1\}$ and the smoother approximation $\phi(\varepsilon) = \tanh(\varepsilon^2)$ were considered in [26, 25].

In the limit $\varepsilon \rightarrow 0$ we have the asymptotic behavior of the partitioned approach, whereas for larger values of ε we have the usual additive approach. The method can be naturally extended to the general multiscale case and provides a consistent discretization also for any value of $\alpha \in [0, 1)$. We refer to [24, 29] for further details. One of the main advantages of this approach is that it results in a convex approximation at different times of the space derivative $p(u)_x$. Therefore, one can use different space discretizations for the derivative appearing at time n and the one at time $n + 1$. Typically, at time n one can choose a standard hyperbolic discretization that works for large values of ε , whereas at time $n + 1$ classical central difference schemes that work in the parabolic limit suffice to avoid a CFL condition of the type $\Delta t = \mathcal{O}(\varepsilon)$. In this sense the function $\phi(\varepsilon)$ can be also interpreted as an interpolation parameter between different fluxes in the evaluation of the space derivatives in (10). The determination of the optimal expression of $\phi(\varepsilon)$ in terms of stability and accuracy is a delicate aspect which is beyond the scope of the present paper.

3. A unified IMEX Runge–Kutta approach. In this section we present a different approach which overcomes some of the drawbacks of the above mentioned methods.

3.1. Description of the method. Again let us consider initially, for simplicity of notation, the case $\alpha = 1$.

We now consider the following discretization for system (1):

$$(15) \quad \begin{aligned} \frac{u^{n+1} - u^n}{\Delta t} &= -v_x^{n+1}, \\ \varepsilon^2 \frac{v^{n+1} - v^n}{\Delta t} &= -\left(p(u^n)_x + v^{n+1} - f(u^n)\right). \end{aligned}$$

Solving the second equation for v^{n+1} one obtains

$$(16) \quad v^{n+1} = \frac{\varepsilon^2}{\varepsilon^2 + \Delta t} v^n - \frac{\Delta t}{\varepsilon^2 + \Delta t} (p(u^n)_x - f(u^n)).$$

Making use of this relation in the first equation, we get

$$\frac{u^{n+1} - u^n}{\Delta t} + \frac{\varepsilon^2}{\varepsilon^2 + \Delta t} v_x^n = \frac{\Delta t}{\varepsilon^2 + \Delta t} (p(u^n)_{xx} - f(u^n)_x).$$

Note that at variance with all the previous approaches, the first equation now uses only two time levels, and the space derivatives all appear at the same time level n . Therefore, we can rewrite the scheme in the equivalent fully explicit form,

$$(17) \quad \begin{aligned} \frac{u^{n+1} - u^n}{\Delta t} + \frac{\varepsilon^2}{\varepsilon^2 + \Delta t} v_x^n + \frac{\Delta t}{\varepsilon^2 + \Delta t} f(u^n)_x &= \frac{\Delta t}{\varepsilon^2 + \Delta t} p(u^n)_{xx}, \\ \frac{v^{n+1} - v^n}{\Delta t} + \frac{1}{\varepsilon^2 + \Delta t} p(u^n)_x &= -\frac{1}{\varepsilon^2 + \Delta t} (v^n - f(u^n)). \end{aligned}$$

In particular, for small values of Δt the scheme (17) corresponds to the system

$$(18) \quad \begin{aligned} u_t + \frac{\varepsilon^2}{\varepsilon^2 + \Delta t} v_x + \frac{\Delta t}{\varepsilon^2 + \Delta t} f(u)_x &= \frac{\Delta t}{\varepsilon^2 + \Delta t} p(u)_{xx} + \mathcal{O}(\Delta t), \\ v_t + \frac{1}{\varepsilon^2 + \Delta t} p(u)_x &= -\frac{1}{\varepsilon^2 + \Delta t} (v - f(u)) + \mathcal{O}(\Delta t), \end{aligned}$$

where we only used

$$\frac{u^{n+1} - u^n}{\Delta t} = u_t + \mathcal{O}(\Delta t), \quad \frac{v^{n+1} - v^n}{\Delta t} = v_t + \mathcal{O}(\Delta t),$$

leaving all other terms.

Note that the left part of system (18) is hyperbolic with characteristic speeds¹

$$(19) \quad \lambda_{\pm}^1(\Delta t, \varepsilon) = \frac{\xi_1}{2} \left(c \pm \sqrt{c^2 + \frac{4\varepsilon^2}{\Delta t^2}} \right),$$

with $\xi_1 = \Delta t/(\varepsilon^2 + \Delta t) \in (0, 1)$, $c = f'(u)$, and for simplicity we have set $p'(u) = 1$.

¹The subscript 1 in (19) indicates $\alpha = 1$.

Now, if $\Delta t \rightarrow 0$ for a fixed ε , system (18) converges to the original system (1) for $\alpha = 1$, and by (19), the characteristic speeds converge to the usual ones, i.e.,

$$\lambda_{\pm}^1(0, \varepsilon) = \pm \frac{1}{\varepsilon}.$$

On the other hand, for a fixed Δt , the characteristic speeds λ_+^1 and λ_-^1 in (19) are, respectively, decreasing and increasing functions of ε and as $\varepsilon \rightarrow 0$ they converge to

$$(20) \quad \lambda_{\pm}^1(\Delta t, 0) = \frac{1}{2} (c \pm |c|).$$

Therefore, if we denote by Δx the space discretization parameter, we obtain the expected hyperbolic CFL condition $\Delta t \leq \Delta x/|c|$.

Concerning the second order derivative on the right-hand side of (18), this induces a stability restriction of type $\Delta t \sim (\Delta x)^2/\xi_1$. In particular, since the discrete system (17) as $\varepsilon \rightarrow 0$ relaxes towards

$$(21) \quad \frac{u^{n+1} - u^n}{\Delta t} + f(u^n)_x = p(u^n)_{xx},$$

in such a limit we have the natural stability condition which links the time step to the square of the mesh space $\Delta t \sim (\Delta x)^2$.

Similarly, in the case when $\alpha \in [0, 1)$, for small values of Δt the scheme applied to (1) corresponds to the system

$$(22) \quad \begin{aligned} u_t + \frac{\varepsilon^{1+\alpha}}{\varepsilon^{1+\alpha} + \Delta t} v_x + \frac{\Delta t}{\varepsilon^{1+\alpha} + \Delta t} f(u)_x &= \frac{\Delta t \varepsilon^{1-\alpha}}{\varepsilon^{1+\alpha} + \Delta t} p(u)_{xx} + \mathcal{O}(\Delta t), \\ v_t + \frac{\varepsilon^{1-\alpha}}{\varepsilon^{1+\alpha} + \Delta t} p(u)_x &= -\frac{1}{\varepsilon^{1+\alpha} + \Delta t} (v - f(u)) + \mathcal{O}(\Delta t). \end{aligned}$$

The left-hand side in (22) now has characteristic speeds

$$(23) \quad \lambda_{\pm}^{\alpha}(\Delta t, \varepsilon) = \frac{\xi_{\alpha}}{2} \left(c \pm \sqrt{c^2 + \frac{4\varepsilon^2}{(\Delta t)^2}} \right),$$

with $\xi_{\alpha} = \Delta t/(\varepsilon^{1+\alpha} + \Delta t) \in [0, 1)$. As before, if we fix ε and send $\Delta t \rightarrow 0$, we obtain the usual characteristic speeds

$$\lambda_{\pm}^{\alpha}(0, \varepsilon) = \pm \frac{1}{\varepsilon^{\alpha}}.$$

The limit behavior of the discrete system now is given by

$$(24) \quad \frac{u^{n+1} - u^n}{\Delta t} + f(u^n)_x = 0,$$

and, similarly to the analysis for $\alpha = 1$, we now observe that the characteristic speed does not diverge as $\varepsilon \rightarrow 0$ since we have

$$\lambda_{\pm}^{\alpha}(\Delta t, 0) = \frac{1}{2} (c \pm |c|).$$

Therefore, we obtain the expected hyperbolic CFL condition $\Delta t \leq \Delta x/|c|$, coming from the hyperbolic part of the system. As before, the stability restriction coming from the parabolic term is $\Delta t \sim \Delta x^2/\xi_{\alpha}$.

3.2. Extension to general IMEX Runge–Kutta schemes. Now we extend the analysis just performed for the simple first order IMEX Euler scheme to a general IMEX Runge–Kutta (RK) scheme.

3.2.1. Notation. An IMEX RK scheme can be represented with a double Butcher tableau,

$$(25) \quad \text{Explicit : } \left. \begin{array}{c} \tilde{c} \\ \tilde{A} \\ \tilde{b}^T \end{array} \right|, \quad \text{Implicit : } \left. \begin{array}{c} c \\ A \\ b^T \end{array} \right|,$$

where $\tilde{A} = (\tilde{a}_{ij})$ is an $s \times s$ lower triangular matrix with zero diagonal entries for an explicit scheme, and, since computational efficiency in most cases is of paramount importance, usually the $s \times s$ matrix $A = (a_{ij})$ for an implicit scheme is restricted to the particular class of diagonally implicit Runge–Kutta (DIRK) methods, i.e., ($a_{ij} = 0$, for $j > i$). In fact, the use of a DIRK scheme is enough to ensure that the explicit part of the scheme term is always evaluated explicitly (see [1, 11, 7]).

The coefficients \tilde{c} and c are given by the usual relation $\tilde{c}_i = \sum_{j=1}^{i-1} \tilde{a}_{ij}$, $c_i = \sum_{j=1}^i a_{ij}$, and the vectors $\tilde{b} = (\tilde{b}_i)_{i=1,\dots,s}$ and $b = (b_i)_{i=1,\dots,s}$ provide the quadrature weights to combine internal stages of the RK method.

The order conditions can be derived as usual by matching the Taylor expansion of the exact and numerical solution; we refer to [1, 11, 32] for more details. Let us mention that from a practical viewpoint, coupling conditions becomes rather severe if one is interested in very high order schemes (say higher than third).

Here we recall the order conditions for IMEX RK schemes up to order $p = 2$ and $p = 3$, under the assumption that $\tilde{c} = c$:

first order (consistency)	$\tilde{b}^T e = 1,$	$b^T e = 1,$
second order	$\tilde{b}c = 1/2,$	$b^T c = 1/2,$
(26)		
third order	$\tilde{b}c^2 = 1/3,$	$b^T c^2 = 1/3,$
	$b^T \tilde{A}c = 1/6,$	$\tilde{b}^T \hat{A}c = 1/6, \quad b^T Ac = 1/6, \quad \tilde{b}^T Ac = 1/6,$

where we denote $e^T = (1, \dots, 1) \in \mathbb{R}^s$, and from the previous relaxation for \tilde{c} and c , we have $\tilde{A}e = \tilde{c}$ and $Ae = c$.

It is useful to characterize the different IMEX schemes we consider in this paper according to the structure of the DIRK method. From [2], we have the following definition.

- DEFINITION 3.1.**
1. We call an IMEX RK method to be of type I or type A (see [32]) if the matrix $A \in \mathbb{R}^{s \times s}$ is invertible, or, equivalently, $a_{ii} \neq 0$, $i = 1, \dots, s$.
 2. We call an IMEX RK method to be of type II or type CK (see [11]) if the matrix A can be written as

$$(27) \quad A = \begin{pmatrix} 0 & 0 \\ a & \hat{A} \end{pmatrix},$$

with $a = (a_{21}, \dots, a_{s1})^T \in \mathbb{R}^{(s-1)}$, and the submatrix $\hat{A} \in \mathbb{R}^{(s-1) \times (s-1)}$ is invertible, or equivalently, $a_{ii} \neq 0$, $i = 2, \dots, s$. In the special case when $a = 0$, $b_1 = 0$, the scheme is said to be of type ARS (see [1]) and the DIRK method is reducible to a method using $s - 1$ stages.

The following definition will also be useful to characterize the properties of the method [6, 8].

DEFINITION 3.2. We call an IMEX RK method implicitly stiffly accurate (ISA) if the corresponding DIRK method is stiffly accurate, namely

$$(28) \quad a_{si} = b_i, \quad i = 1, \dots, s.$$

If, in addition, the explicit method satisfies

$$(29) \quad \tilde{a}_{si} = \tilde{b}_i, \quad i = 1, \dots, s - 1,$$

the IMEX RK method is said to be globally stiffly accurate (GSA).

The definitions of ISA follow naturally from the fact that s -stage implicit RK methods for which $a_{si} = b_i$ for $i = 1, \dots, \nu$ are called *stiffly accurate* (see [19] for details). A ν -stage explicit RK method for which $\tilde{a}_{si} = \tilde{b}_i$ for $i = 1, \dots, s - 1$ is called FSAL (*first same as last*, see [20] for details). Note that FSAL methods have the advantage that they require only $s - 1$ function evaluations per time step, because the last stage of step n coincides with the first stage of step $n + 1$.

Therefore, an IMEX RK scheme is GSA if the implicit scheme is stiffly accurate and the explicit scheme is FSAL. We observe that this definition states also that the numerical solution of a GSA IMEX RK scheme coincides exactly with the last internal stage of the scheme.

3.2.2. The unified IMEX RK setting. Let us consider system (1), and again for simplicity of notation, we set $\alpha = 1$. The unified IMEX RK approach that generalizes first order scheme (15) corresponds to compute first the internal stages U and V ,

$$(30) \quad \begin{aligned} U &= u^n e - \Delta t A V_x, \\ V &= v^n e - \frac{\Delta t}{\varepsilon^2} \tilde{A}(p(U)_x - f(U)) - \frac{\Delta t}{\varepsilon^2} A V, \end{aligned}$$

and then the numerical solution

$$(31) \quad \begin{aligned} u^{n+1} &= u^n - \Delta t b^T V_x, \\ v^{n+1} &= v^n - \frac{\Delta t}{\varepsilon^2} \tilde{b}^T (p(U)_x - f(U)) - \frac{\Delta t}{\varepsilon^2} b^T V, \end{aligned}$$

where $f(U)$ and $p(U)$ are the vectors with component $f(U)_i = f(U^i)$ and $p(U)_i = p(U^i)$, respectively. Solving the second equation for V in (30) with $\zeta = \varepsilon^2/\Delta t$, one obtains

$$(32) \quad V = (\zeta I + A)^{-1} \left(\zeta v^n e - \tilde{A}(p(U)_x - f(U)) \right).$$

Substituting this relation in the first equation, we have that the resulting IMEX RK scheme may be written as

$$(33) \quad \begin{aligned} \frac{U - u^n e}{\Delta t} + \zeta A(\zeta I + A)^{-1} e v_x^n + A(\zeta I + A)^{-1} \tilde{A} f(U)_x &= A(\zeta I + A)^{-1} \tilde{A} p(U)_{xx}, \\ \frac{V - v^n e}{\Delta t} + \frac{1}{\varepsilon^2} \tilde{A} p(U)_x &= -\frac{1}{\varepsilon^2} \left(A V - \tilde{A} f(U) \right), \end{aligned}$$

$$(34) \quad \begin{aligned} \frac{u^{n+1} - u^n}{\Delta t} + \zeta b^T (\zeta I + A)^{-1} e v_x^n + b^T (\zeta I + A)^{-1} \tilde{A} f(U)_x &= b^T (\zeta I + A)^{-1} \tilde{A} p(U)_{xx}, \\ \frac{v^{n+1} - v^n}{\Delta t} + \frac{1}{\varepsilon^2} \tilde{b}^T p(U)_x &= -\frac{1}{\varepsilon^2} (b^T V - \tilde{b}^T f(U)). \end{aligned}$$

Then setting $B = (\zeta I + A)^{-1}$ for small values of Δt , from (34) we get the system

$$(35) \quad \begin{aligned} u_t + \zeta b^T B e v_x + b^T B \tilde{A} f(U)_x &= b^T B \tilde{A} p(U)_{xx} + \mathcal{O}(\Delta t), \\ v_t + \frac{1}{\varepsilon^2} \tilde{b}^T p(U)_x &= -\frac{1}{\varepsilon^2} (b^T V - \tilde{b}^T f(U)) + \mathcal{O}(\Delta t). \end{aligned}$$

Now, we rewrite $f(U)_x = f'(U)U_x$ and $p(U)_x = p'(U)U_x$, where $f'(U)$ and $p'(U)$ are diagonal matrices with elements $f'(U)_{ii} = f'(U^i)$ and $p'(U)_{ii} = p'(U^i)$, respectively. Furthermore, for simplicity we assume $f'(U^i) = c$ and $p'(U^i) = 1$.

From the IMEX RK stages (33) we have

$$(36) \quad U = u_n e - \varepsilon^2 A B e v_x^n - \Delta t c A B \tilde{A} U_x + \Delta t A B \tilde{A} U_{xx},$$

and using the fact that $U = u^n e + \mathcal{O}(\Delta t)$ and $\tilde{b}^T e = 1$ (consistency of the IMEX RK scheme), we can write the hyperbolic part in (35) as

$$(37) \quad \begin{aligned} u_t + \zeta b^T B e v_x + c b^T B \tilde{A} e u_x &= \mathcal{O}(\Delta t), \\ v_t + \frac{1}{\varepsilon^2} u_x &= \mathcal{O}(\Delta t). \end{aligned}$$

By computing the eigenvalues of the hyperbolic part we obtain

$$(38) \quad \Lambda_{\pm}^1(\Delta t, \varepsilon) = \frac{1}{2} \left(c b^T B \tilde{A} e \pm \sqrt{(c b^T B \tilde{A} e)^2 + 4 \frac{b^T B e}{\Delta t}} \right).$$

Next, we show that the above characteristic speeds are limited. Here we need to assume that the scheme is GSA. In fact,

$$(39) \quad b^T B e = b^T (\zeta I + A)^{-1} e = \begin{cases} 1 & \text{for } \zeta \rightarrow 0, \\ \sim \frac{1}{\zeta} & \text{for } \zeta \rightarrow \infty, \end{cases}$$

where for the first case using the ISA property we get $b^T A^{-1} e = e_s^T e = 1$ (here $e_s^T = (0, \dots, 0, 1) \in \mathbb{R}^s$), whereas for the second case, we note that for the consistency of the scheme $b^T e = 1$. On the other hand,

$$(40) \quad b^T B \tilde{A} e = b^T (\zeta I + A)^{-1} \tilde{A} e = \begin{cases} 1 & \text{for } \zeta \rightarrow 0, \\ \sim \frac{1}{2\zeta} & \text{for } \zeta \rightarrow \infty, \end{cases}$$

where for the first case using the GSA property we get $b^T A^{-1} \tilde{A} e = e_s^T \tilde{A} e = \tilde{b}^T e = 1$, whereas for the second case we note that the quantity $b^T \tilde{A} e$ is a number, and if we assume that the scheme is a second order accurate one, this gives $b^T \tilde{A} e = 1/2$, by (26).

As a consequence we have

$$(41) \quad \Lambda_{\pm}^1(\Delta t, 0) = \frac{1}{2} \left(c \pm \sqrt{c^2 + \frac{4}{\Delta t}} \right), \quad \Lambda_{\pm}^1(0, \varepsilon) = \pm \frac{1}{\varepsilon},$$

and therefore, the CFL condition, in the limit $\varepsilon \rightarrow 0$, becomes

$$(42) \quad \Delta t \leq \left(\frac{|c|}{2} + \sqrt{\frac{c^2}{4} + \frac{1}{\Delta t}} \right)^{-1} \Delta x = \frac{2\sqrt{\Delta t}}{|c|\sqrt{\Delta t} + \sqrt{c^2\Delta t + 4}} \Delta x.$$

Now, if $\Delta t \ll 1$, we get from

$$\sqrt{\Delta t} \leq \frac{2}{|c|\sqrt{\Delta t} + \sqrt{c^2\Delta t + 4}} \Delta x$$

the parabolic time step restriction $\Delta t \sim \Delta x^2$.

Finally, we prove that the scheme (33)–(34) in the limit case $\varepsilon \rightarrow 0$ is a consistent discretization of the limit equation (6), i.e., the scheme is AP.

From (32) we get

$$V = \zeta A^{-1} v^n e - A^{-1} (I - \zeta A^{-1}) \tilde{A} (f(U) - p(U)_x) + \mathcal{O}(\zeta^2),$$

and substituting in the numerical solution v^{n+1} we obtain

$$\zeta v^{n+1} = \zeta (1 - b^T A^{-1} e) v^n + (b^T A^{-1} \tilde{A} - \tilde{b}^T) (U_x - f(U)) - \zeta b^T A^{-2} \tilde{A} (f(U) - p(U)_x) + \mathcal{O}(\zeta^2).$$

Consistency, as $\zeta \rightarrow 0$, implies $(b^T A^{-1} \tilde{A} - \tilde{b}^T) = 0$, which is satisfied if the scheme is GSA, because in this case $b^T = e_s^T A$, $\tilde{b}^T = e_s^T \tilde{A}$; therefore, $1 - b^T A^{-1} e = 0$ and $b^T A^{-1} \tilde{A} - \tilde{b}^T = e_s^T \tilde{A} - \tilde{b}^T = 0$. Then we have

$$v^{n+1} = -b^T A^{-2} \tilde{A} (f(U) - p(U)_x) = e_s^T A^{-1} \tilde{A} (f(U) - p(U)_x)$$

with

$$V = -A^{-1} \tilde{A} (f(U) - p(U)_x).$$

Similarly, from (33) we have for the U internal stages

$$\frac{U - u^n}{\Delta t} = -\zeta v_x^n e + \tilde{A} (p(U)_x - f(U))_x - \zeta A^{-1} \tilde{A} (p(U)_x - f(U)) + \mathcal{O}(\zeta^2),$$

and for the numerical solution

$$\frac{u^{n+1} - u^n}{\Delta t} = -\zeta b^T v_x^n e + b^T A^{-1} \tilde{A} (p(U)_x - f(U))_x - \zeta b^T A^{-2} \tilde{A} (p(U)_x - f(U))_x + \mathcal{O}(\zeta^2).$$

Therefore, for $\zeta \rightarrow 0$, this leads to

$$(43) \quad \begin{aligned} U &= u^n e + \Delta t \tilde{A} (p(U)_x - f(U))_x, \\ u^{n+1} &= u^n + \Delta t b^T A^{-1} \tilde{A} (p(U)_x - f(U))_x. \end{aligned}$$

Assuming that the IMEX RK scheme is GSA, the term $b^T A^{-1} \tilde{A} = e_s^T \tilde{A} = \tilde{b}^T$, and, as $\varepsilon \rightarrow 0$, the scheme relaxes to the explicit one, i.e.,

$$(44) \quad \begin{aligned} \frac{U - u^n e}{\Delta t} + \tilde{A} f(U)_x &= \tilde{A} p(U)_{xx}, \\ \frac{u^{n+1} - u^n}{\Delta t} + \tilde{b}^T f(U)_x &= \tilde{b}^T p(U)_{xx}. \end{aligned}$$

Generalization to the case $\alpha \in [0, 1]$. In the case $\alpha \in [0, 1]$, analogous computations show that the characteristic speeds of the hyperbolic part are given by

$$(45) \quad \Lambda_{\pm}^{\alpha}(\Delta t, \varepsilon) = \frac{1}{2} \left(cb^T B \tilde{A} e \pm \sqrt{\left(cb^T B \tilde{A} e \right)^2 + 4 \frac{\varepsilon^{1-\alpha}}{\Delta t} b^T B e} \right),$$

where here $\zeta = \varepsilon^{1+\alpha}/\Delta t$. We have

$$\Lambda_{\pm}^{\alpha}(\Delta t, 0) = \frac{1}{2} (c \pm |c|), \quad \Lambda_{\pm}^{\alpha}(0, \varepsilon) = \pm \frac{1}{\varepsilon^{\alpha}}.$$

A similar analysis performed in this case shows that

$$\begin{aligned} U &= u^n e - \Delta t \tilde{A} f(U)_x + \Delta t \varepsilon^{(1-\alpha)} \tilde{A} (p(U)_{xx} + \mathcal{O}(\xi^2)), \\ u^{n+1} &= u^n - \Delta t \tilde{b}^T f(U)_x + \Delta t \varepsilon^{(1-\alpha)} \tilde{b}^T p(U)_{xx} + \mathcal{O}(\xi^2). \end{aligned}$$

As $\varepsilon \rightarrow 0$ we get the explicit RK scheme for system (4),

$$(46) \quad \begin{aligned} \frac{U - u^n e}{\Delta t} + \tilde{A} f(U)_x &= 0, \\ \frac{u^{n+1} - u^n}{\Delta t} + \tilde{b}^T f(U)_x &= 0. \end{aligned}$$

All the previous results can be stated by the following theorem.

THEOREM 3.3. *If the IMEX RK scheme (30)–(31) applied to (1) satisfies the GSA property, then, as $\varepsilon \rightarrow 0$, it becomes the explicit RK scheme characterized by the pair (\tilde{A}, \tilde{w}) applied to the limit convection-diffusion equation (6) for $\alpha = 1$ and to the limit scalar conservation law (3) for $\alpha \in [0, 1]$.*

Some remarks are in order.

Remark 1. • The advantage of formulating the unified IMEX RK approach in the form (33)–(34) is that we can now adopt different space discretizations for the various terms appearing in the scheme. Typically, we use classical hyperbolic-type schemes, like WENO, for the space derivatives characterizing the hyperbolic part (which now has finite characteristic speeds) and centered discretization for the second order term characterizing the asymptotic parabolic behavior.

- If the IMEX RK scheme satisfies the GSA property, and the numerical solution is the same as the last stage, then $V^s = v^{n+1}$, and observing that $\tilde{b}_s = 0$, from the second equation of (34), we have

$$\frac{v^{n+1} - v^n}{\Delta t} + \frac{1}{\varepsilon^2} \sum_{i=1}^{s-1} \tilde{b}_i p(U^j)_x = -\frac{1}{\varepsilon^2} \left(\sum_{i=1}^{s-1} (b_i V^i - \tilde{b}_i f(U^i)) + b_s v^{n+1} \right).$$

Solving for v^{n+1} , after some algebra, the equation can be written as

$$\begin{aligned} \frac{v^{n+1} - v^n}{\Delta t} + \frac{1}{\varepsilon^2 + b_s \Delta t} \sum_{i=1}^{s-1} \tilde{b}_i p(U^j)_x \\ = -\frac{1}{\varepsilon^2 + b_s \Delta t} \left(\sum_{i=1}^{s-1} (b_i V^i - \tilde{b}_i f(U^i)) + b_s v^n \right). \end{aligned}$$

Assuming $p'(u) = 1$ and using the fact that $U = u^n e + \mathcal{O}(\Delta t)$, we can now write the hyperbolic part in (33) as

$$(47) \quad \begin{aligned} u_t + \zeta b^T B e v_x + c b^T B \tilde{A} e u_x &= \mathcal{O}(\Delta t), \\ v_t + \frac{1}{\varepsilon^2 + a_{ss} \Delta t} u_x &= \mathcal{O}(\Delta t). \end{aligned}$$

Therefore, the characteristic speeds read

$$(48) \quad \Lambda_{\pm}^1(\Delta t, \varepsilon) = \frac{1}{2} \left(c b^T B \tilde{A} e \pm \sqrt{\left(c b^T B \tilde{A} e \right)^2 + 4 \frac{\zeta b^T B e}{\varepsilon^2 + a_{ss} \Delta t}} \right),$$

and now when $\varepsilon \rightarrow 0$, as in the first order case discussed in section 3, we get

$$\Lambda_{\pm}^1(\Delta t, 0) = \frac{1}{2} (c \pm |c|).$$

4. Removing the parabolic stiffness. Although the final schemes developed in the previous section will work independently on ε and α , for small values of ε they relax to an explicit RK scheme originating a time step restriction of the type $\Delta t \approx \Delta x^2 / \varepsilon^{1-\alpha}$, for $\alpha \in (0, 1]$. Therefore, for small ε , only the case when $\alpha = 1$ poses stability restriction. For this reason, we shall consider $\alpha = 1$ in this subsection.

The natural idea here is to treat the term $p(u)_x$ in (1) implicitly and to observe that in the limit case, i.e., $\varepsilon \rightarrow 0$, the IMEX RK scheme relaxes to an IMEX RK scheme for the limit convection-diffusion equation (6), where the diffusion term is now evaluated implicitly. Compared to similar schemes presented in [6, 8, 9] this new approach has the advantage in that it is not based on a penalization technique and therefore avoids the difficult problem of the optimal determination of the penalization parameter (see [6]).

The unified IMEX RK scheme for system (1) now reads

$$(49) \quad \begin{aligned} U &= u^n e - \Delta t A V_x, \\ V &= v^n e + \frac{\Delta t}{\varepsilon^2} \tilde{A} f(U) - \frac{\Delta t}{\varepsilon^2} A(V + p(U)_x), \end{aligned}$$

and

$$(50) \quad \begin{aligned} u^{n+1} &= u^n - \Delta t b^T V_x, \\ v^{n+1} &= v^n + \frac{\Delta t}{\varepsilon^2} \tilde{b}^T f(U) - \frac{\Delta t}{\varepsilon^2} b^T (V + p(U)_x). \end{aligned}$$

Now, solving the second equation in (49) for V , one obtains

$$(51) \quad V = (\zeta I + A)^{-1} \left(\zeta v^n e + \tilde{A} f(U) - A p(U)_x \right),$$

where $\zeta = \varepsilon^2 / \Delta t$. Using this relation in the first equation of (49), we get for the internal stages

$$(52) \quad \begin{aligned} \frac{U - u^n}{\Delta t} + \zeta A (\zeta I + A)^{-1} v^n e &= A (\zeta I + A)^{-1} (A p(U)_x - \tilde{A} f(U))_x, \\ \frac{V - v^n}{\Delta t} + \frac{1}{\varepsilon^2} \tilde{A} f(U) &= -\frac{1}{\varepsilon^2} A (V + p(U)_x), \end{aligned}$$

and similarly for the numerical solution,

$$(53) \quad \begin{aligned} \frac{u^{n+1} - u^n}{\Delta t} + \zeta b^T (\zeta I + A)^{-1} v_x^n e &= b^T (\zeta I + A)^{-1} (Ap(U)_x - \tilde{A}f(U))_x, \\ \frac{v^{n+1} - v^n}{\Delta t} + \frac{1}{\varepsilon^2} \tilde{b}^T f(U) &= -\frac{1}{\varepsilon^2} b^T (V + p(U)_x). \end{aligned}$$

Then setting $B = (\zeta I + A)^{-1}$ for small values of Δt , from (53) we get the system

$$(54) \quad \begin{aligned} u_t + \zeta b^T B e v_x + b^T B \tilde{A} f(U)_x &= b^T B A p(U)_{xx} + \mathcal{O}(\Delta t), \\ v_t + \frac{1}{\varepsilon^2} b^T p(U)_x &= -\frac{1}{\varepsilon^2} (b^T V - \tilde{b}^T f(U)) + \mathcal{O}(\Delta t), \end{aligned}$$

which is similar to (35), except that now A and b^T appear in front of $p(U)$ terms in place of \tilde{A} and \tilde{b} , respectively. Therefore, we have the same characteristic speeds as in the unified IMEX RK approach presented in the previous section, and the same conclusions on the hyperbolic CFL condition hold true.

Concerning the AP property, in the limit $\zeta \rightarrow 0$ one has from (51)

$$V = -p(U)_x + A^{-1} \tilde{A} f(U),$$

and by the GSA property, i.e., $b^T A^{-1} \tilde{A} = e_s^T \tilde{A} = \tilde{b}^T$, we get from (53)

$$v^{n+1} = -e_s^T (p(U)_x - A^{-1} \tilde{A} f(U)).$$

Thus, scheme (52)–(53) becomes an IMEX RK scheme for the convection-diffusion equation (6),

$$(55) \quad \begin{aligned} \frac{U - u^n e}{\Delta t} + \tilde{A} f(U)_x &= A p(U)_{xx}, \\ \frac{u^{n+1} - u^n}{\Delta t} + \tilde{b}^T f(U)_x &= b^T p(U)_{xx}. \end{aligned}$$

Clearly, scheme (55) is a consistent approximation of the limit equation (6), where now the diffusion term is evaluated implicitly. Therefore, the CFL condition of such a scheme is uniquely determined by the hyperbolic restriction $\Delta t \sim \Delta x$. A similar analysis in the case when $\alpha \in [0, 1)$ for scheme (49)–(50) under the GSA assumption produces the explicit RK scheme

$$(56) \quad \begin{aligned} U &= u^n - \Delta t \tilde{A} f(U)_x, \\ u^{n+1} &= u^n - \Delta t \tilde{b}^T \tilde{A} f(U)_x. \end{aligned}$$

Therefore we can summarize the results in the following theorem.

THEOREM 4.1. *If the IMEX RK scheme (49)–(50), applied to (1) for $\alpha = 1$, satisfies the GSA property, then as $\varepsilon \rightarrow 0$, it becomes the IMEX RK method characterized by the pairs (\tilde{A}, \tilde{b}) and (A, b) for the limit convection-diffusion equation (6). Otherwise, for $\alpha \in [0, 1)$ the IMEX RK scheme as $\varepsilon \rightarrow 0$ yields the explicit RK method characterized by the pair (\tilde{A}, \tilde{b}) for the limit scalar conservation law (4).*

5. Numerical applications. In this section we present numerical results that confirm the validity of the new approach presented in section 4. In all tests we used the last approach described in section 4, so that we remove the parabolic restriction

in the limit of small ε and $\alpha = 1$. All the numerical examples presented here refer to the IMEX RK schemes reported in the appendix. We shall use the notation $\text{NAME}(\nu, \sigma, p)$, with the triplet (ν, σ, p) , where ν, σ , and p represent, respectively, the number of explicit function evaluations, the number of implicit function evaluations, and the order of accuracy.

In order to avoid spurious numerical oscillations arising near discontinuities of the solutions, we use interpolating nonoscillatory algorithms, like the WENO method [36]. In these numerical tests, as emphasized in Remark 1, we use classical hyperbolic-type schemes, like finite difference discretization with WENO reconstruction, for the space derivatives characterized by the hyperbolic part, while for the second order term $p(u)_{xx}$ we used the standard 2th and 4th order finite difference technique. Note that when we consider the third order IMEX RK scheme we use fourth order finite difference to discretize the term $p(u)_{xx}$ except at the nearby boundary points where a third order formula was implemented, and this guarantees we will achieve a global third order.

In all our numerical results, we take $\Delta t = \lambda_{CFL} \Delta x$ in all regimes. The precise choice of λ_{CFL} is reported in the figure captions.

As a mathematical model for our numerical experiments, we consider the Ruijgrook–Wu model of the discrete kinetic theory of rarefied gases. The model describes a two-speed gas in one space dimension and corresponds to the system [17, 25, 35]

$$(57) \quad \begin{cases} M \partial_t f^+ + \partial_x f^+ = -\frac{1}{\text{Kn}}(a f^+ - b f^- - c f^+ f^-), \\ M \partial_t f^- - \partial_x f^- = \frac{1}{\text{Kn}}(a f^+ - b f^- - c f^+ f^-), \end{cases}$$

where f^+ and f^- denote the particle density distribution at time t , position x , and with velocity $+1$ and -1 , respectively. Here Kn is the Knudsen number, M is the Mach number of the system, and a, b , and c are positive constants which characterize the microscopic interactions. The local (Maxwellian) equilibrium is defined by

$$(58) \quad f^+ = \frac{b f^-}{a - c f^-}.$$

The macroscopic variables for the model are the density u and momentum v , defined by

$$(59) \quad u = f^+ + f^-, \quad v = (f^+ - f^-)/M.$$

The nondimensional multiscale problem is obtained taking $M = \varepsilon^\alpha$, $\text{Kn} = \varepsilon$. The Reynolds number of the system is then defined according to $Re = M/\text{Kn} = 1/\varepsilon^{1-\alpha}$, as usual. The model, as we will see, has a nice feature: it provides nontrivial limit behaviors for various values of α , including the corresponding compressible Euler ($\alpha = 0$) limit and the incompressible Euler ($\alpha \in (0, 1)$) and Navier–Stokes ($\alpha = 1$) limits.

Test 1. Diffusive scaling in the linear case. For this numerical test we consider the case $\alpha = 1$ (namely $M = \text{Kn} = \varepsilon$) with $c = 0$, $a = (1 - A\varepsilon)/2$, and $b = (1 + A\varepsilon)/2$ in the right-hand side of (57).

Adding and subtracting the two equations in (57) one obtains the following macro-

scopic equations for u and v :

$$(60) \quad \begin{cases} \partial_t u + \partial_x v = 0, \\ \partial_t v + \frac{1}{\varepsilon^2} \partial_x u = -\frac{1}{\varepsilon^2} (v - Au). \end{cases}$$

In the limit $\varepsilon \rightarrow 0$ the second equation relaxes to the local equilibrium

$$v = Au - \frac{\partial u}{\partial x},$$

and substituting in the first equation this gives the limiting advection-diffusion equation

$$u_t + Au_x = u_{xx}.$$

Next, we fix $A = 1$ and observe that the limiting advection-diffusion equation admits the exact solution

$$(61) \quad u(x, t) = e^{-t} \sin(x - t), \quad v(x, t) = e^{-t} (\sin(x - t) - \cos(x - t))$$

on the domain $[-\pi, \pi]$ with periodic boundary conditions. We start to consider as initial conditions (61) at $t = 0$, and choose $\varepsilon = 10^{-6}$ with final time $T = 0.1$. The numerical results are compared with (61) at $t = T$. Relative errors and convergence orders are reported in Tables 1–3. In order to check the temporal order of convergence of these schemes, Δx decreases with the time step Δt according to the CFL condition $\Delta t = 0.5 \Delta x$. In the tables we show the order of convergence as

$$p = \log_2(\|E_{\Delta t}\|_{\infty} / \|E_{\Delta t/2}\|_{\infty}),$$

with $E_{\Delta t}$ the relative error computed with time step Δt . We consider the error obtained with $N = 40$ time steps up to $N = 640$ time steps in the interval $[0, T]$. We observe that the classical order of the methods ARS(1,1,1), CK(2,2,2), and BPR(3,4,3) is maintained in the limit case for the density u ; see Table 1. We omit the convergence results of the ARS(2,2,2) scheme (74) since they are essentially the same as those obtained with the CK(2,2,2) scheme.

Typically, classical schemes like ARS(2,2,2), CK(2,2,2), and BPR(3,4,3), which satisfy only the GSA property, have few numbers of internal stages but maintain, in the limit $\varepsilon \rightarrow 0$, the order in time only for the u -component, while for the v -component they do not guarantee even the consistency [8]. As an example, we report the convergence table for the variable v in Table 2 for the CK(2,2,2) scheme (75), and we observe that we do not obtain the correct classical order of accuracy for v in the limit case $\varepsilon \rightarrow 0$.

The reason for the lack of consistency in the algebraic component v is that these classical schemes do not satisfy the additional order conditions (72) (see the appendix) that guarantee the consistency of the scheme and the order up to 2 for the variable v . As a comparison, we construct a new scheme, BPR(4,4,2), that satisfies the additional order conditions (72), and in Table 3 we observe the correct convergence rate for both components, u and v . Furthermore, in Figure 1, we also compare the numerical solutions (star points) for u (u -num) and v (v -num) obtained with the second order ARS(2,2,2) scheme (74) and BPR(4,4,2) scheme. In the same figure, the exact solution is plotted by a continuous line. Note again that the new scheme BPR(4,4,2) shows the correct behavior for the v variable.

TABLE 1

Test 1. Convergence rates for the density u with $\varepsilon = 10^{-6}$.

Method	N	L_∞ error	Order
ARS(1,1,1)	40	$6.4800e-03$	--
ARS(1,1,1)	80	$3.5082e-03$	0.8853
ARS(1,1,1)	160	$1.9203e-03$	0.8694
ARS(1,1,1)	320	$9.6447e-04$	0.9935
ARS(1,1,1)	640	$4.8457e-04$	0.9930
CK(2,2,2)	40	$1.4911e-04$	--
CK(2,2,2)	80	$3.9405e-05$	1.9199
CK(2,2,2)	160	$1.1356e-05$	1.7949
CK(2,2,2)	320	$2.8331e-06$	2.0030
CK(2,2,2)	640	$7.0874e-07$	1.9991
BPR(3,4,3)	40	$5.8318e-06$	--
BPR(3,4,3)	80	$7.8658e-07$	2.8903
BPR(3,4,3)	160	$1.2095e-07$	2.7012
BPR(3,4,3)	320	$1.5297e-08$	2.9831
BPR(3,4,3)	640	$1.9253e-09$	2.9901

Of course there are some advantages and disadvantages in considering additional order conditions (72). The advantage is that they guarantee the correct order in the limit case ($\varepsilon \rightarrow 0$) for both variables. On the other hand, to construct schemes that satisfy (72) requires a larger number of internal stages due to these extra order conditions.

TABLE 2

Test 1. Convergence rates for v for the scheme CK(2, 2, 2) with $\varepsilon = 10^{-6}$.

Method	N	L_∞ v-error	Order of v
CK(2,2,2)	40	$1.3156e-02$	--
CK(2,2,2)	80	$1.4897e-02$	-0.1793
CK(2,2,2)	160	$1.1520e-03$	3.6928
CK(2,2,2)	320	$1.2584e-03$	-0.1274
CK(2,2,2)	640	$1.2877e-03$	-0.0332

TABLE 3

Test 1. Convergence rates for u and v for the scheme (76) with $\varepsilon = 10^{-6}$.

Method	N	L_∞ u-error	Order u	L_∞ v-error	Order v
BPR(4,4,2)	40	$1.9129e-04$	--	$2.8704e-04$	--
BPR(4,4,2)	80	$4.9963e-05$	1.9368	$8.0261e-05$	1.8385
BPR(4,4,2)	160	$1.4374e-05$	1.7974	$2.0603e-05$	1.9618
BPR(4,4,2)	320	$3.5895e-06$	2.0016	$5.2702e-06$	1.9669
BPR(4,4,2)	640	$9.0120e-07$	1.9939	$1.4011e-06$	1.9113

Next, we consider a Riemann problem with initial data

$$(62) \quad \begin{cases} u_L = 4.0, & v_L = 0, & -10 < x < 0, \\ u_R = 2.0, & v_R = 0, & 0 < x < 10, \end{cases}$$

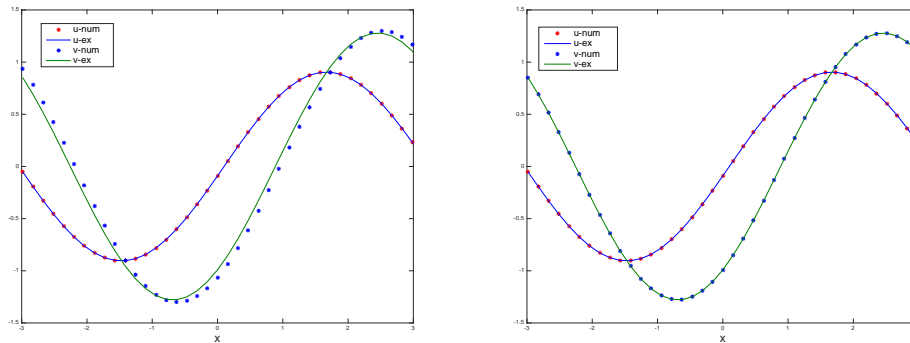


FIG. 1. Test 1. Comparison between classical ARS(2,2,2) scheme (left) and the BPR(4,4,2) scheme (right) with $N = 40$ and $\Delta t = 0.5\Delta x$.

and inflow and outflow boundary conditions. The exact solution for the limit advection-diffusion equation is

$$(63) \quad u(x, t) = \frac{1}{2}(u_L + u_R) + \frac{1}{2}(u_L - u_R)\operatorname{erf}\left(\frac{t-x}{2\sqrt{t}}\right),$$

where $\operatorname{erf}(x)$ denotes the error function. We take $\Delta x = 0.2$ and the final time $T = 3.0$. In Figure 2 we compare the numerical solutions computed by schemes SP(1,1,1), BPR(2,4,4), and BPR(3,3,5) for the mass density in the intermediate regime ($\varepsilon = 0.5$) with a reference solution obtained with $\Delta x = 0.001$ and in the diffusive one ($\varepsilon = 10^{-6}$) with the analytical solution (63). As we can see, the numerical results for the different schemes are in excellent agreement with the reference and analytical solutions using a hyperbolic time step $\Delta t = 0.5\Delta x$.

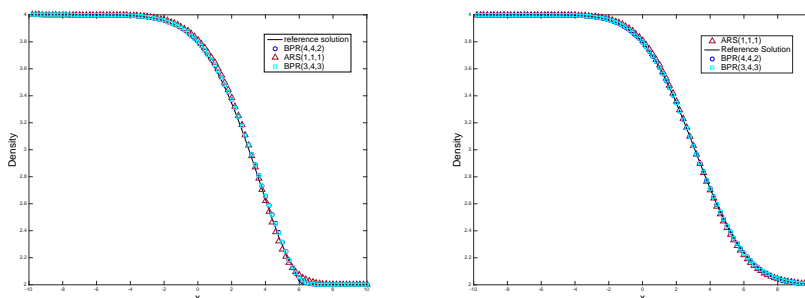


FIG. 2. Test 1. Solution of problem (60) with initial data (62), $\Delta x = 0.2$, and $\Delta t = 0.5\Delta x$ for the density u . Left: The rarefied regime $\varepsilon = 0.5$. Right: The parabolic regime $\varepsilon = 10^{-6}$.

Test 2. Multiscale limit in the nonlinear case. Here we consider the nonlinear Ruijgrok–Wu model (57) with interaction parameters $c = \varepsilon^\alpha$ and $a = b = 1/2$. Adding and subtracting the two equations in (57) one obtains the following macro-

scopic equations for u and v :

$$(64) \quad \begin{cases} \partial_t u + \partial_x v = 0, \\ \partial_t v + \frac{1}{\varepsilon^{2\alpha}} \partial_x u = \frac{1}{\varepsilon^{1+\alpha}} \left\{ -v + \frac{1}{2} (u^2 - \varepsilon^{2\alpha} v^2) \right\}. \end{cases}$$

For small values of ε the model behavior can be derived by the Chapman–Enskog expansion and for $\alpha > 1/3$ is characterized by the viscous Burgers equation

$$(65) \quad \begin{aligned} v &= \frac{1}{2} u^2 - \varepsilon^{1-\alpha} \partial_x u + \mathcal{O}(\varepsilon^{2\alpha}), \\ \partial_t u + \partial_x \left(\frac{u^2}{2} \right) &= \varepsilon^{1-\alpha} \partial_{xx} u + \mathcal{O}(\varepsilon^{2\alpha}). \end{aligned}$$

To avoid dealing with nonlinear solvers, the IMEX schemes have been applied by keeping implicit only the linear term v in the right-hand side of (64) and leaving explicit the quadratic term v^2 . For this reason, for small values of ε we will restrict to $\alpha \in (1/3, 1]$.

We consider two different initial conditions. In the first case we take $\alpha = 1$ and two local Maxwellian equilibrium characterized by

$$(66) \quad \begin{cases} u_L = 2.0, & v_L = 0, & -10 < x < 0, \\ u_R = 1.0, & v_R = 0, & 0 < x < 10, \end{cases}$$

with $v = [(1 + u^2 \varepsilon^2)^{1/2} - 1] / \varepsilon^2$.

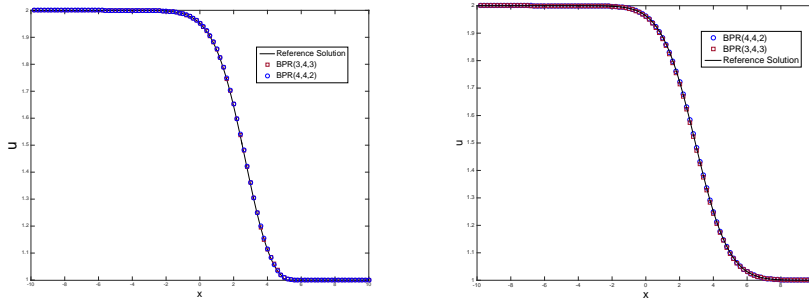


FIG. 3. Test 2. Numerical solutions of problem (64) for $\alpha = 1$ with initial conditions (66) at $T = 2.0$ and $\Delta t = 0.5 \Delta x$. Left: The rarefied regime for u with $\varepsilon = 0.4$. Right: The parabolic regime for u with $\varepsilon = 10^{-6}$.

We show in Figure 3 the numerical solution for u using BPR(4,4,2) and BPR(3,4,3) schemes in the rarefied ($\varepsilon = 0.4$) and parabolic ($\varepsilon = 10^{-6}$) regimes with $\Delta x = 0.2$ at the final time $T = 0.2$. The solution of both schemes is in very good agreement with the reference solution computed with $\Delta x = 0.04$.

The last test case that we consider is the propagation of an initial square wave. The initial profile is specified as

$$(67) \quad u = 1.0, \quad v = 0.0 \quad \text{for } |x| < 0.125, \quad u = v = 0 \quad \text{for } |x| > 0.125,$$

with reflecting boundary conditions, i.e., $v = 0, u_x = 0$ on the boundary.

This test is taken from [30]. Because of the different notation, the parameters ε and α adopted in [30], which we denote by $\tilde{\varepsilon}$, $\tilde{\alpha}$, have a different meaning in our paper. The correspondence between $\tilde{\varepsilon}$, $\tilde{\alpha}$ and ε , α adopted in the present paper is

$$\varepsilon = \tilde{\varepsilon}^{(1+\tilde{\alpha})}, \quad \alpha = \frac{1}{1+\tilde{\alpha}}.$$

We integrate the equations over $[-0.5, 0.5]$ with 200 spatial cells. We use the BPR(3,4,3) scheme (77). In Figure 4 we plot the behavior of the system for various regimes. The

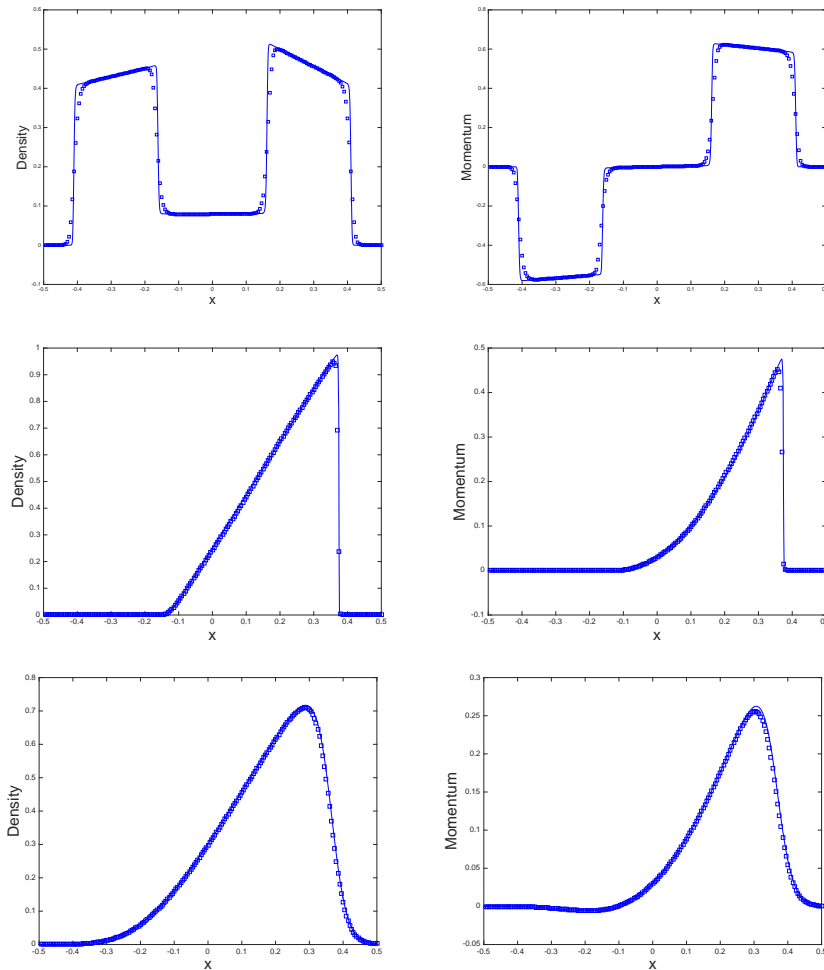


FIG. 4. Test 2. Numerical solutions of system (64) with initial conditions (67) for the mass density u (left) and the momentum v (right) in the rarefied regime (top panels) with $\varepsilon = 0.7$, $\alpha = 1$, and $\Delta t = 0.0025$, $\Delta x = 0.005$ at time $T = 0.2$. In the hyperbolic regime $\varepsilon = 10^{-12}$, with $\alpha = 2/3$ (mid panels), and parabolic regime $\varepsilon = 10^{-10}$ with $\alpha = 4/5$ (bottom panels) and $\Delta t = 0.004$ (i.e., $\Delta t = 0.8\Delta x$) at time $T = 0.5$.

panels on the top are obtained in the rarefied regime, with $\varepsilon = 0.7$ and $\alpha = 1$ (corresponding to $\tilde{\varepsilon} = 0.7$ and $\tilde{\alpha} = 0$ in [30]) at time $T = 0.2$. We observe that in the rarefied regime no oscillation appears and the scheme describes well the behavior of the system.

The middle panels illustrate the results obtained in the case of the hyperbolic regime $\varepsilon = 10^{-12}$ and $\alpha = 2/3$ (corresponding to $\tilde{\varepsilon} = 10^{-8}$ and $\tilde{\alpha} = 0.5$ in [30]) at time $T = 0.5$. Notice the propagation of the right moving shock.

The bottom panels present the results for the parabolic scaling $\varepsilon = 10^{-10}$ and $\alpha = 4/5$ (corresponding to $\tilde{\varepsilon} = 10^{-8}$ and $\tilde{\alpha} = 0.25$ in [30]) at time $T = 0.5$. As we see, the scheme perfectly captures all regimes, even if it is underresolved for small values of ε .

The numerical solutions for the mass density u and momentum v are computed in the rarefied regime and in the diffusive regime with $\Delta t = 0.5\Delta x$ and are depicted with a reference solution obtained using fine grids with $\Delta x = 0.001$.

Test 3. Multiscale space varying limit in the nonlinear case. Finally, we consider the multiscale relaxation system of the previous section in the case where the parameter $\alpha = \alpha(x) \in (1/3, 1]$ depends on the space variable. Therefore, the limit behavior of the system may depend on the particular region of the computational domain. For this test, we consider $\alpha(x) \in [1/2, 1]$.

Now we apply our schemes to system (64) considering two different cases of the varying α number. The domain is chosen to be $x \in [-0.5, 0.5]$. In the first case α increases smoothly from a small value α_0 to $\mathcal{O}(1)$ by the formula

$$(68) \quad \alpha(x) = \alpha_0 + 0.25(1 + \tanh(20(x + 0.1)))$$

with $\alpha_0 = 0.5$. In the second case we consider the function α which contains a discontinuity

$$(69) \quad \begin{cases} \alpha_L = 0.5, & -0.5 < x < 0, \\ \alpha_R = 1.0, & 0 < x < 0.5. \end{cases}$$

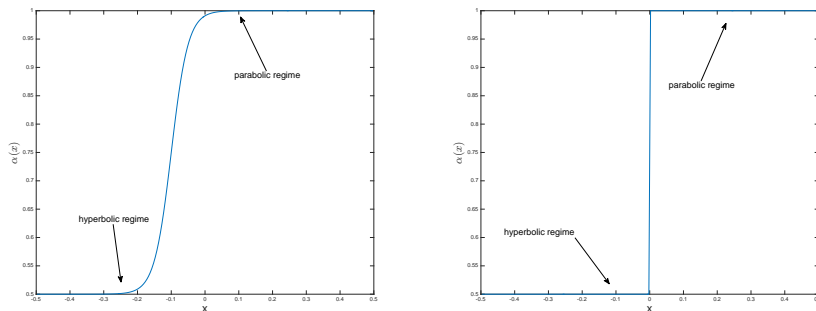


FIG. 5. Test 3. Space varying $\alpha(x)$. Left: the smooth profile (68). Right: the discontinuous profile (69).

The two different scenarios for α are depicted in Figure 5. The initial profile is specified by (67) with reflecting boundary conditions, and we fix $\varepsilon = 10^{-8}$ and $\Delta t = 0.5\Delta x$. Here we use the BPR(3,4,3) scheme. The reference solutions are computed using a fine grid with $\Delta x = 0.001$. The results are depicted up to time $T = 0.05$ (left) and $T = 0.18$ (right). In Figure 6 we observe that the scheme is able to capture the correct behavior of the reference solution even in this test case.

6. Conclusions. In this work we have developed a new IMEX RK approach that is capable of correctly capturing the asymptotic behavior of hyperbolic balance laws

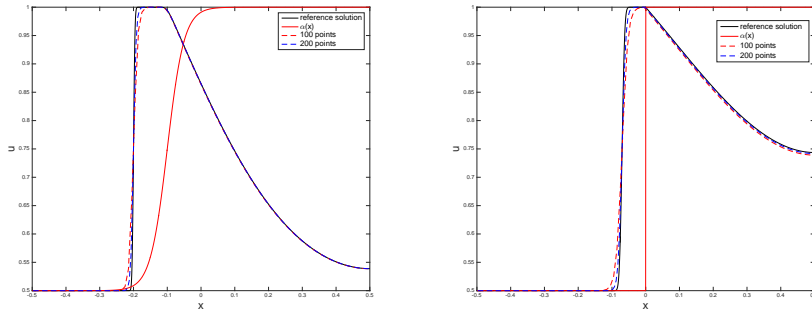


FIG. 6. Test 3. For $\varepsilon = 10^{-8}$, the left and right pictures show the behavior of the component u in the two different cases of α .

with relaxation under different kinds of scaling. Previous IMEX RK schemes were designed to deal specifically with one kind of scaling, either hyperbolic [7, 10, 22, 32] or parabolic [6, 21, 25, 29], whereas the present schemes are robust enough to be able to deal with both scalings. Related approaches were presented in [8, 24, 27, 30].

From a physical viewpoint, these scaling limits correspond to the classical fluid-dynamic scalings in the kinetic theory of rarefied gases that lead from the Boltzmann equation to its compressible and incompressible limits. Several numerical tests for a simple kinetic model which possess different asymptotic limits have confirmed the validity of the present approach. In the near future, we hope to extend this class of IMEX RK schemes to the full Boltzmann equation by adopting the penalization techniques developed in [15, 16].

Appendix A. IMEX RK schemes. In order to achieve higher than first order accuracy in time for GSA IMEX RK schemes, we need to observe first that there are no second order GSA IMEX RK methods of type I with $s = 3$, i.e., with three stages [6]. Thus, to construct a second order GSA IMEX RK scheme we consider the following proposition [6].

PROPOSITION A.1. *The only type of second order GSA IMEX RK scheme with three levels $s = 3$ that satisfies the classical second order conditions (26) is the type II, where $c_i = \tilde{c}_i$ for all $i = 2, \dots, s - 1$, with $c_1 = 0$ and $c_s = 1$.*

As usual, order conditions are obtained by matching the Taylor expansion of the exact solution and the numerical one, up to terms of the prescribed order. In the relaxed case, i.e., $\varepsilon \rightarrow 0$, system (1) for $\alpha = 1$ reduces to

$$(70) \quad v = -p(u)_x + f(u), \quad u_t + f(u)_x = p(u)_{xx}.$$

The unified IMEX RK approach described in section 4 provides a scheme that converges to an explicit-implicit scheme for the limit convection-diffusion equation in (70). Performing the same analysis as proposed in [8] for system (1), we obtain for the u -component the classical order conditions, while some additional order conditions for the v -component are required in order to have consistency and maintain the classical order in the limit case. We recall that the GSA assumption of the method guarantees that the IMEX RK scheme relaxes at the same IMEX RK scheme when $\varepsilon \rightarrow 0$, but to maintain the order of accuracy of the scheme in the limit we must impose some additional order conditions.

Below we list these new additional order conditions that the v -component must satisfy up to second order.

consistency	$b^T A^{-2} \tilde{A}e = 1,$
first order	$b^T A^{-2} \tilde{A}c = 1, \quad b^T A^{-2} \tilde{A}\tilde{c} = 1,$
(71) second order	$b^T A^{-2} \tilde{A}c^2 = 1, \quad b^T A^{-2} \tilde{A}\tilde{c}^2 = 1, \quad b^T A^{-2} \tilde{A}\tilde{c}c = 1, \quad b^T A^{-2} \tilde{A}c\tilde{c} = 1,$ $b^T A^{-2} \tilde{A}Ac = 1/2, \quad b^T A^{-2} \tilde{A}A\tilde{c} = 1/2,$ $b^T A^{-2} \tilde{A}\tilde{A}c = 1/2, \quad b^T A^{-2} \tilde{A}\tilde{A}\tilde{c} = 1/2.$

Note that in order to reduce the number of the additional order conditions, we require that $\tilde{c} = c$. This assumption considerably simplifies the number of coupling conditions.

(72)	consistency	$b^T A^{-2} \tilde{A}e = 1,$
	first order	$b^T A^{-2} \tilde{A}c = 1,$
	second order	$b^T A^{-2} \tilde{A}c^2 = 1, \quad b^T A^{-2} \tilde{A}Ac = 1/2, \quad b^T A^{-2} \tilde{A}\tilde{A}c = 1/2.$

Finally, we present the different IMEX RK schemes, up to order three, used in our numerical tests. Below, these schemes are represented by the usual double Butcher tableau. On the left we have the explicit part and on the right the implicit part of the IMEX schemes. All of the schemes satisfy the GSA property, but only the new scheme BPR(4, 4, 2) satisfies the additional order conditions (72).

- First order ARS(1, 1, 1) scheme:

$$(73) \quad \begin{array}{c|cc} 0 & 0 & 0 \\ \hline 1 & 1 & 0 \\ \hline & 1 & 0 \end{array} \quad \begin{array}{c|cc} 0 & 0 & 0 \\ \hline 1 & 0 & 1 \\ \hline & 0 & 1 \end{array}.$$

- Second order ARS(2, 2, 2) scheme [1]:

$$(74) \quad \begin{array}{c|ccc} 0 & 0 & 0 & 0 \\ \hline \gamma & \gamma & 0 & 0 \\ 1 & \delta & 1 - \delta & 0 \\ \hline & \delta & 1 - \delta & 0 \end{array} \quad \begin{array}{c|ccc} 0 & 0 & 0 & 0 \\ \hline \gamma & 0 & \gamma & 0 \\ 1 & 0 & 1 - \gamma & \gamma \\ \hline & 0 & 1 - \gamma & \gamma \end{array},$$

where $\gamma = 1 - 1/\sqrt{2}$ and $\delta = 1 - 1/2\gamma$.

- Second order CK(2, 2, 2) scheme [11]:

$$(75) \quad \begin{array}{c|ccc} 0 & 0 & 0 & 0 \\ \hline 2/3 & 2/3 & 0 & 0 \\ 1 & 1/4 & 3/4 & 0 \\ \hline & 1/4 & 3/4 & 0 \end{array} \quad \begin{array}{c|ccc} 0 & 0 & 0 \\ \hline -1/3 + \sqrt{2}/2 & 1 - \sqrt{2}/2 & 0 \\ 3/4 - \sqrt{2}/4 & -3/4 + 3\sqrt{2}/4 & 1 - \sqrt{2}/2 \\ \hline & 3/4 - \sqrt{2}/4 & -3/4 + 3\sqrt{2}/4 & 1 - \sqrt{2}/2 \end{array}.$$

- Second order BPR(4, 4, 2) scheme:

$$(76) \quad \begin{array}{c|ccccc} 0 & 0 & 0 & 0 & 0 \\ \hline 1/4 & 1/4 & 0 & 0 & 0 \\ 1/4 & 13/4 & -3 & 0 & 0 \\ 3/4 & 1/4 & 0 & 1/2 & 0 \\ 1 & 0 & 1/3 & 1/6 & 1/2 \\ \hline & 0 & 1/3 & 1/6 & 1/2 \end{array} \quad \begin{array}{c|ccccc} 0 & 0 & 0 & 0 & 0 \\ \hline 1/4 & 0 & 1/4 & 0 & 0 \\ 1/4 & 0 & 0 & 1/4 & 0 \\ 3/4 & 0 & 1/24 & 11/24 & 1/4 \\ 1 & 0 & 11/24 & 1/6 & 1/8 \\ \hline & 0 & 11/24 & 1/6 & 1/8 \end{array}.$$

- Third order BPR(3, 4, 3) scheme [6]:

$$(77) \begin{array}{c|cccccc|cccccc} & 0 & 0 & 0 & 0 & 0 & 0 & 0 & 0 & 0 & 0 & 0 \\ & 1 & 1 & 0 & 0 & 0 & 0 & 1 & 1/2 & 1/2 & 0 & 0 & 0 \\ & 2/3 & 4/9 & 2/9 & 0 & 0 & 0 & 2/3 & 5/18 & -1/9 & 1/2 & 0 & 0 \\ & 1 & 1/4 & 0 & 3/4 & 0 & 0 & 1 & 1/2 & 0 & 0 & 1/2 & 0 \\ & 1 & 1/4 & 0 & 3/4 & 0 & 0 & 1 & 1/4 & 0 & 3/4 & -1/2 & 1/2 \\ \hline & & 1/4 & 0 & 3/4 & 0 & 0 & & 1/4 & 0 & 3/4 & -1/2 & 1/2 \end{array}.$$

Acknowledgments. The authors are grateful to Professors M. Lemou and G. Dimarco for helpful observations.

REFERENCES

- [1] U. M. ASCHER, S. J. RUUTH, AND R. J. SPITERI, *Implicit-explicit Runge-Kutta methods for time-dependent partial differential equations*, Appl. Numer. Math., 25 (1997), pp. 151–167, [https://doi.org/10.1016/S0168-9274\(97\)00056-1](https://doi.org/10.1016/S0168-9274(97)00056-1).
- [2] S. BOSCARINO, *Error analysis of IMEX Runge-Kutta methods derived from differential-algebraic systems*, SIAM J. Numer. Anal., 45 (2007), pp. 1600–1621, <https://doi.org/10.1137/060656929>.
- [3] S. BOSCARINO, *On an accurate third order implicit-explicit Runge-Kutta method for stiff problems*, Appl. Numer. Math., 59 (2009), pp. 1515–1528, <https://doi.org/10.1016/j.apnum.2008.10.003>.
- [4] C. BARDOS, C. D. LEVERMORE, AND F. GOLSE, *Fluid dynamic limit of kinetic equations II: Convergence proofs for the Boltzmann equations*, Comm. Pure Appl. Math., 46 (1993), pp. 667–753, <http://dx.doi.org/10.1002/cpa.3160460503>.
- [5] S. BOSCARINO AND L. PARESCHI, *On the asymptotic properties of IMEX Runge-Kutta schemes for hyperbolic balance laws*, J. Comput. Appl. Math., 316 (2017), pp. 60–73, <https://doi.org/10.1016/j.cam.2016.08.027>.
- [6] S. BOSCARINO, L. PARESCHI, AND G. RUSSO, *Implicit-explicit Runge-Kutta schemes for hyperbolic systems and kinetic equations in the diffusion limit*, SIAM J. Sci. Comput., 35 (2013), pp. A22–A51, <https://doi.org/10.1137/110842855>.
- [7] S. BOSCARINO AND G. RUSSO, *On a class of uniformly accurate IMEX Runge-Kutta schemes and applications to hyperbolic systems with relaxation*, SIAM J. Sci. Comput., 31 (2009), pp. 1926–1945, <https://doi.org/10.1137/080713562>.
- [8] S. BOSCARINO AND G. RUSSO, *Flux-explicit IMEX Runge-Kutta schemes for hyperbolic to parabolic relaxation problems*, SIAM J. Numer. Anal., 51 (2013), pp. 163–190, <https://doi.org/10.1137/110850803>.
- [9] S. BOSCARINO, P. LE FLOCH, AND G. RUSSO, *High-Order asymptotic-preserving methods for fully nonlinear relaxation problems*, SIAM J. Sci. Comput., 36 (2014), pp. A377–A395, <https://doi.org/10.1137/120893136>.
- [10] R. E. CAFLISCH, S. JIN, AND G. RUSSO, *Uniformly accurate schemes for hyperbolic systems with relaxation*, SIAM J. Numer. Anal., 34 (1997), pp. 246–281, <https://doi.org/10.1137/S0036142994268090>.
- [11] M. H. CARPENTER AND C. A. KENNEDY, *Additive Runge-Kutta schemes for convection-diffusion-reaction equations*, Appl. Numer. Math., 44 (2003), pp. 139–181, [https://doi.org/10.1016/S0168-9274\(02\)00138-1](https://doi.org/10.1016/S0168-9274(02)00138-1).
- [12] C. CERCIGNANI, R. ILLNER, AND M. PULVIRENTI, *The Mathematical Theory of Dilute Gases*, Appl. Math. Sci. 106, Springer-Verlag, New York, 1994.
- [13] G. Q. CHEN, C. D. LEVERMORE, AND T. P. LIU, *Hyperbolic conservation laws with stiff relaxation terms and entropy*, Comm. Pure and App. Math., 47 (1994), pp. 787–830, <https://doi.org/10.1002/cpa.3160470602>.
- [14] C. CERCIGNANI, *The Boltzmann Equation and Its Applications*, Appl. Math. Sci. 67, Springer-Verlag, New York, 1988.
- [15] G. DIMARCO AND L. PARESCHI, *Asymptotic-preserving IMEX Runge-Kutta methods for nonlinear kinetic equations*, SIAM J. Numer. Anal., (2013), pp. 1064–1087, <https://doi.org/10.1137/12087606X>.
- [16] F. FILBET AND S. JIN, *A class of asymptotic preserving schemes for kinetic equations and related problems with stiff sources*, J. Comput. Phys., 229 (2010), pp. 7625–7648, <https://doi.org/10.1016/j.jcp.2010.06.017>.

- [17] E. GABETTA AND B. PERTHAME, *Scaling limits for the Ruijgrook-Wu model of the Boltzmann equation*, Math. Meth. Appl. Sci., 24 (2001), pp. 949–967, <https://doi.org/10.1002/mma.251>.
- [18] E. GABETTA, L. PARESCHI, AND G. TOSCANI, *Relaxation schemes for nonlinear kinetic equations*, SIAM J. Numer. Anal., 34 (1997), pp. 2168–2194, <https://doi.org/10.1137/S0036142995287768>.
- [19] E. HAIRER AND G. WANNER, *Solving Ordinary Differential Equations II: Stiff and Differential Algebraic Problems*, Springer Ser. Comput. Math. 14, 2nd revised ed., Springer-Verlag, Berlin, Heidelberg, 1996.
- [20] E. HAIRER, S. P. NORSETT, AND G. WANNER, *Solving Ordinary Differential Equation I: Nonstiff Problems*, Springer Ser. Comput. Math. 8, 2nd revised ed., Springer-Verlag, Berlin, Heidelberg, 1993.
- [21] A. KLAR, *An asymptotic-induced scheme for nonstationary transport equations in the diffusive limit*, SIAM J. Numer. Anal., 35 (1998), pp. 1073–1094, <https://doi.org/10.1137/S0036142996305558>.
- [22] S. JIN, *Runge-Kutta methods for hyperbolic conservation laws with stiff relaxation terms*, J. Comput. Phys., 122 (1995), pp. 51–65, <https://doi.org/10.1006/jcph.1995.1196>.
- [23] S. JIN AND C. D. LEVERMORE, *Numerical schemes for hyperbolic conservation laws with stiff relaxation terms*, J. Comput. Phys., 126 (1996), pp. 449–467, <https://doi.org/10.1006/jcph.1996.0149>.
- [24] S. JIN AND L. PARESCHI, *Asymptotic-preserving (AP) schemes for multiscale kinetic equations: A unified approach*, in Hyperbolic Problems: Theory, Numerics, Applications, Internat. Ser. Numer. Math. 141, Birkhäuser, Basel, 2001, pp. 573–582.
- [25] S. JIN, L. PARESCHI, AND G. TOSCANI, *Diffusive relaxation schemes for multiscale discrete-velocity kinetic equations*, SIAM J. Numer. Anal., 35 (1998), pp. 2405–2439, <https://doi.org/10.1137/S0036142997315962>.
- [26] S. JIN, L. PARESCHI, AND G. TOSCANI, *Uniformly accurate diffusive relaxation schemes for multiscale transport equations*, SIAM J. Numer. Anal., 38 (2000), pp. 913–936, <https://doi.org/10.1137/S0036142998347978>.
- [27] M. LEMOU AND L. MIEUSSSENS, *A new asymptotic preserving scheme based on micro-macro formulation for linear kinetic equations in the diffusion limit*, SIAM J. Sci. Comput., 31 (2008), pp. 334–368, <https://doi.org/10.1137/07069479X>.
- [28] T. P. LIU, *Hyperbolic conservation laws with relaxation*, Comm. Math. Phys., 108 (1987), pp. 153–175, <http://projecteuclid.org/euclid.cmp/1104116362>.
- [29] G. NALDI AND L. PARESCHI, *Numerical schemes for kinetic equations in diffusive regimes*, Appl. Math. Lett., 11 (1998), pp. 29–35, [https://doi.org/10.1016/S0893-9659\(98\)00006-8](https://doi.org/10.1016/S0893-9659(98)00006-8).
- [30] G. NALDI AND L. PARESCHI, *Numerical schemes for hyperbolic systems of conservation laws with stiff diffusive relaxation*, SIAM J. Numer. Anal., 37 (2000), pp. 1246–1270, <https://doi.org/10.1137/S0036142997328810>.
- [31] L. PARESCHI, *Characteristic-based numerical schemes for hyperbolic systems with nonlinear relaxation*, Rend. Circ. Mat. di Palermo, II, 57 (1998), pp. 375–380.
- [32] L. PARESCHI AND G. RUSSO, *Implicit-explicit Runge-Kutta schemes and applications to hyperbolic systems with relaxations*, J. Sci. Comput., 25 (2005), pp. 129–155, <https://doi.org/10.1007/s10915-004-4636-4>.
- [33] R. B. PEMBER, *Numerical methods for hyperbolic conservation laws with stiff relaxation I. Spurious solutions*, SIAM J. Appl. Math., 53 (1993), pp. 1293–1330, <https://doi.org/10.1137/0153062>.
- [34] P. L. ROE AND M. ARORA, *Characteristic-based schemes for dispersive waves. I. The method of characteristics for smooth solutions*, Numer. Methods Partial Differential Equations, 9 (1993), pp. 459–505, <https://doi.org/10.1002/num.1690090502>.
- [35] W. RUIJGROOK AND T. T. WU, *A completely solvable model of the nonlinear Boltzmann equation*, Phys. A, 113 (1982), pp. 401–416, [https://doi.org/10.1016/0378-4371\(82\)90147-9](https://doi.org/10.1016/0378-4371(82)90147-9).
- [36] C. W. SHU, *Essentially non-oscillatory and weighted essentially non-oscillatory schemes for hyperbolic conservation laws*, in Advanced Numerical Approximation of Nonlinear Hyperbolic Equations, Springer, Berlin, 1998, pp. 325–432.